

Supra-amphiphilic aggregates formed by *p*-sulfonatocalix[4]arenes and the antipsychotic drug chlorpromazine

Cite this: *Soft Matter*, 2014, 10, 2253

Zhanbin Qin, Dong-Sheng Guo, Xiao-Ning Gao and Yu Liu*

We report here a supramolecular strategy to directly assemble the small molecular antipsychotic drug chlorpromazine (CPZ) into nanostructures, induced by *p*-sulfonatocalix[4]arene (SC4A) and *p*-sulfonatocalix[4]arene tetraheptyl ether (SC4AH), with high drug loading efficiencies of 61% and 46%, respectively. The binary host–guest assembly process was monitored using optical transmittance measurements, and the size and morphology of these two kinds of supra-amphiphilic assemblies were identified using a combination of light scattering and high-resolution transmission electron microscopy, which showed solid spherical micelles. This strategy presents new opportunities for the development of high loading drug-containing carriers with easy processability for drug delivery.

Received 13th November 2013
Accepted 10th December 2013

DOI: 10.1039/c3sm52866a

www.rsc.org/softmatter

Introduction

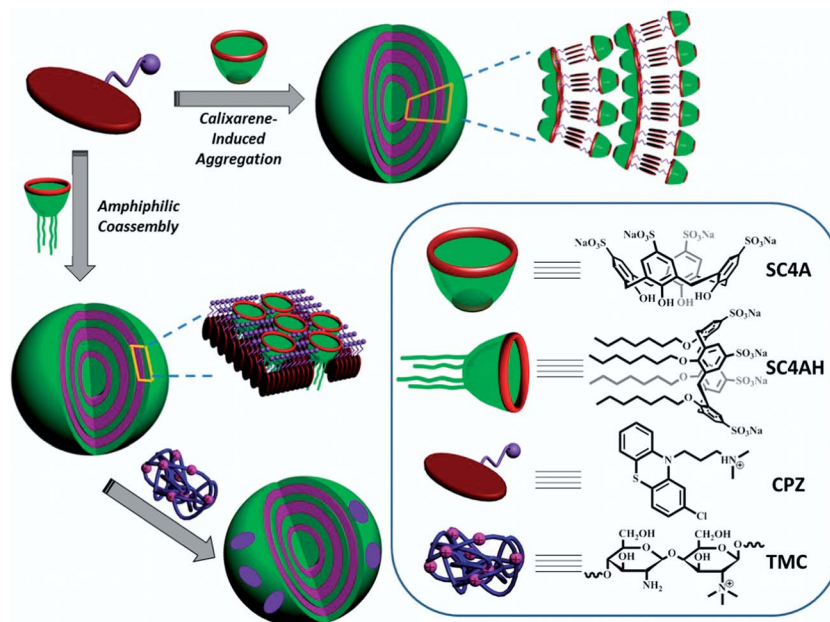
Self-assembled nanocarriers are attracting increasing attention due to their wide range of applications in various practical fields; among them, one of the foremost applications is drug delivery. Several kinds of assemblies such as liposomes,¹ polymers,² dendrimers,³ and inorganic nanoparticles⁴ have been proposed as drug carriers. Common drug delivery approaches consist of a drug encapsulated by a suitable nanocarrier.⁵ However, there are inherent difficulties in achieving a quantitative and high drug loading per carrier (typically less than 10%). In contrast with encapsulation, conjugation to a polymeric carrier *via* a liable linker, which must be designed to chemically cleave selectively at the therapeutic target under specific biological conditions (temperature, pH, redox potential, enzyme) in order to release the drug molecules, presents a higher drug loading approach. Nevertheless, it should also be acknowledged that the synthetic route for these polymer-conjugates is tedious more often than not. Furthermore, the linkers could not be ruptured completely under the required physiological conditions resulting in incomplete drug release.⁶ Alternatively, the non-covalent coassembly of drugs with carrier components represents a robust avenue for drug delivery, where the drug molecule itself acts as an essential subunit leading to a well-defined assembly. The aforementioned disadvantages are therefore addressed from the viewpoints of improving the loading efficiency and avoiding tedious syntheses. Hedrick and Yang recently reported the formation of structures through the coassembly of a stereocontrolled block copolymer mixture with

paclitaxel. The morphology of the assemblies changed into elongated fiber-like hierarchical structures from spherical structures after the addition of paclitaxel. The loading content of paclitaxel reached 30–60%.⁷ However, such a coassembly approach is less explored, possibly due to the fact that most drug molecules do not tend to undergo self-assembly.

Phenothiazine compounds are one of significant amphiphilic molecules and are commonly used in clinical medicine as antipsychotic and tranquilizer drugs.⁸ One of the most widely studied phenothiazine derivatives is chlorpromazine hydrochloride (CPZ), which consists of a hydrophobic nitrogen-containing heterocycle bound to a short chain containing a charged amino group (Scheme 1). It can self-assemble at a critical concentration, forming micelle-like structures, which undergo temperature- and concentration-dependent phase transitions.⁹ Therefore, CPZ could be utilized as an ideal model drug molecule for coassembly.

Calixarenes are macrocyclic oligomers made of phenol units linked by methylene bridges.¹⁰ They can be readily functionalized at the phenolic hydroxyl groups (lower rim) and at the *para* positions (upper rim), and they give rise to a wide range of structural derivatives. Calixarene chemistry was initially directed toward the design of host compounds with receptor abilities. However, the versatility of calixarenes is not limited to this, and when properly functionalized, they can be applied in various areas such as the self-assembly of monolayers¹¹ and nanoparticles,¹² and the formation of molecular machines,¹³ dendrimers¹⁴ and amphiphiles.¹⁵ Calixarene-based amphiphiles can be obtained by introducing hydrophilic groups at one rim and hydrophobic groups at the opposite rim.¹⁶ The conformation adopted by the calixarene is a crucial factor in regulating the aggregation behavior and the cone shaped conformation is ideal for the formation of spherical micelles.^{16b} Besides

Department of Chemistry, State Key Laboratory of Elemento-Organic Chemistry, Nankai University, Collaborative Innovation Center of Chemical Science and Engineering, Tianjin 300071, P. R. China. E-mail: yuliu@nankai.edu.cn



Scheme 1 Principle of coassembly of an amphiphilic drug with calixarenes.

calixarene-based amphiphiles, a series of calixarene-based supra-amphiphiles were established by us and by others. These are amphiphiles that are formed on the basis of calixarene host-guest interactions.¹⁷ The construction of calixarene-based supra-amphiphiles is by means of calixarene-induced aggregation (CIA): complexation with *p*-sulfonatocalixarenes promotes the aggregation of aromatic or amphiphilic molecules by lowering the critical aggregation concentration (CAC), enhancing the aggregate stability, and regulating the degree of order in the aggregates.¹⁸

Our interest in developing calixarene-based (supra-) amphiphiles has led us to research the application of stimuli-responsive drug delivery systems, where drug molecules are encapsulated by host-guest binary vesicles, and then released when the vehicles are disrupted by stimuli, such as temperature, redox, additives, and enzymes.¹⁹ Herein, we wish to report the coassembly of an amphiphilic drug with calixarenes, aiming to improve the drug loading efficiency by minimizing the use of inactive materials. Two different routes were concurrently taken: one was the CIA approach afforded by the 1 : *n* complexation of *p*-sulfonatocalix[4]arene (SC4A) with CPZ; the other was the amphiphilic coassembly between anionic *p*-sulfonatocalix[4]arene tetraheptyl ether (SC4AH) and cationic CPZ.

Experimental

General

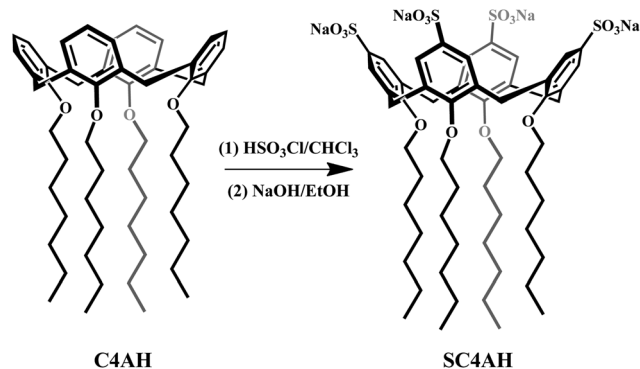
Chlorpromazine Hydrochloride (CPZ) was purchased from TCI. Trimethylated chitosan (TMC $\geq 70\%$) was purchased from Sigma-Aldrich. 4-Phenolsulfonic sodium was purchased from Acros. All of the above were used without further purification. The NMR spectra were recorded using a Bruker AV400 spectrometer in the indicated solvents. Coupling constant values (*J*)

are in Hertz (Hz). The following abbreviations were used for signal multiplicities: s, singlet; d, doublet; and t, triplet. The elemental analysis was recorded using a Perkin-Elmer 2400C instrument.

Synthesis

Calix[4]arene tetraheptyl ether (C4AH)²⁰ was synthesized and purified according to the procedures reported previously.

p-Sulfonatocalix[4]arene tetraheptyl ether (SC4AH): a solution of 3.0 g (3.67 mmol) C4AH in 50.0 mL of CHCl_3 was stirred under argon at ice bath temperature for 30 min. Then 1.1 mL (16.10 mmol dissolved in 60.0 mL of CHCl_3) of HSO_3Cl was added. The mixture was stirred at 0 °C for another 3 h and then concentrated. The residue was dissolved in 100.0 mL of anhydrous EtOH. After, a solution of 735 mg (18.36 mmol) NaOH in anhydrous EtOH was then added and the mixture was stirred for 30 min. After centrifugation the resulting white precipitate was recrystallized from water yielding 3.3 g (73%) of SC4AH



Scheme 2 Synthesis of SC4AH.

(Scheme 2). ^1H NMR (400 MHz, D_2O): $\delta = 7.14$ (s, 8H), 3.76 (t, $J = 201.4$ Hz, 24H), 1.84 (s, 8H), 1.21 (d, $J = 22.8$ Hz, 24H), 0.75 (s, 12H). ^{13}C NMR (100 MHz, D_2O): $\delta = 13.83$ (CH_3), 22.75 (CH_2), 26.33 (CH_2), 29.80 (CH_2), 30.36 (CH_2), 32.17 (CH_2), 75.69 (CH_2), 126.06 (CH), 134.51 (C), 137.41 (C), 158.05 (C). Elemental analysis: calculated for $\text{C}_{56}\text{H}_{76}\text{Na}_4\text{O}_{16}\text{S}_4$: C = 54.89%, H = 6.25%; found: C = 54.96%, H = 6.41%

p-Sulfonatocalix[4]arene (SC4A),²¹ 4-(heptyloxy)benzenesulfonate sodium²² and 1,4-dimethyldiazabicyclo[2.2.2]octane iodide (DBO)²³ were synthesized and purified according to the procedures reported previously and identified using ^1H NMR spectroscopy in D_2O , and elemental analysis.

Determination of CPZ loading in nanoparticles

SC4A-CPZ nanoparticles were prepared as follows: a certain amount of CPZ was added to a solution containing SC4A, and then water was added until the volume of the solution reached 100 mL. The ultimate concentrations of CPZ and SC4A were 150 and 37.5 μM respectively. Subsequently, the prepared nanoparticles were purified by ultracentrifugation (13 000 rpm for 20 min). The resulting precipitates were dried under vacuum and their CPZ loading was calculated from the molar ratio of CPZ to SC4A in a DMSO- d_6 solution by integrating the ^1H NMR signals of aromatic resonances of CPZ and SC4A. The CPZ loading in the SC4AH-CPZ nanoparticles was determined using the same method. The ultimate concentrations of CPZ and SC4AH in solution were 75 and 25 μM respectively.

Electrical conductivity

The electrical conductivity of the solutions was measured using a conductivity meter (INESA Scientific Instrument Co., Ltd., Shanghai, China) at 25 $^\circ\text{C}$.

UV/Vis spectroscopy

The optical transmittance of the aqueous solution was measured in a quartz cell (light path 10 mm) using a Shimadzu UV-3600 spectrophotometer equipped with a PTC-348WI temperature controller.

Isothermal titration calorimetry (ITC)

A thermostated and fully computer-operated isothermal calorimetry (VP-ITC) instrument, purchased from Microcal Inc., Northampton, MA, was used for all microcalorimetric experiments. All microcalorimetric titrations were performed in aqueous solution at atmospheric pressure and 298.15 K. Each solution was de-gassed and thermostated using a ThermoVac accessory before the titration experiment. Twenty-eight successive injections were made for the titration experiment. A constant volume (10 μL per injection) of SC4AH solution was injected, using a 0.250 mL syringe, into the reaction cell (1.4227 mL) charged with redistilled water.

High-resolution TEM measurements

High-resolution TEM images were acquired using a high-resolution TEM (Tecnai G² F20 microscope, FEI) equipped with

a CCD camera (Orius 832, Gatan) operating at an accelerating voltage of 200 kV. The sample for TEM measurements was prepared by dropping the solution onto a copper grid. The grid was then air-dried.

DLS measurements

The sample solution for DLS measurements was prepared by filtering the solution through a 450 nm Millipore filter into a clean scintillation vial. The samples were examined on a laser light scattering spectrometer (BI-200SM) equipped with a digital correlator (TurboCorr) at 636 nm at a scattering angle of 90 $^\circ$. The hydrodynamic radius (R_h) was determined by dynamic light scattering experiments, and the radius of gyration (R_g) was obtained from static light scattering data at different scattering angles.

Results and discussion

In addition to a vast series of natural amphiphiles, a number of synthetic amphiphiles have been designed including macrocycle-based amphiphiles.²⁴ Calixarenes serve as a kind of robust macrocyclic scaffold that results in novel artificial amphiphiles due to their facile modification. Their intrinsic cone shape is the prerequisite for high curvature amphiphilic aggregation.²⁵ Their relatively rigid framework can enhance the stability of amphiphilic aggregation.^{19c} Calixarene amphiphiles consist of multiple lipophilic groups at one rim and multiple hydrophilic groups at the other rim, which are covalently linked by methylene bridges, representing a type of preorganized cyclic oligomer of amphiphiles. From the viewpoint of structural characteristics, they incorporate both gemini-type and bola-type amphiphiles into a single molecule. Taking the preorganized framework and cavity binding property into account, calixarene amphiphiles are envisaged as a new candidate to build desired amphiphilic assemblies with improved stability and fascinating diverse applications.⁶⁻⁹

In the present work, we focus our attention on *p*-sulfonatocalixarene-based (supra-) amphiphiles. *p*-Sulfonatocalixarenes are one of the most significant calixarene derivatives as their benign water-solubility, robust binding capability and satisfactory biocompatibility,²⁶ mean that they have been extensively applied in the fields of biology and pharmacology.²⁷ Aiming to fabricate an amphiphilic assembly, on one hand, *p*-sulfonatocalixarenes have been demonstrated to generate supra-amphiphiles by complexation-induced aggregation;¹⁸ on the other hand, *p*-sulfonatocalixarenes modified at the lower rim with alkyl chains can form amphiphilic assemblies with special recognition sites (calixarene cavity) on their outer-layer surface, which could be further non-covalently coronated and hierarchically assembled.

Due to their commercial availability and the convenience of their syntheses as well as modification, we herein employed the smallest analogue, SC4A and its heptylation derivative SC4AH as the building hosts. Their non-covalent interactions with the amphiphilic drug CPZ were examined, and then two amphiphilic assemblies were fabricated *via* different assembling

models: (1) supra-amphiphile directed by SC4A-induced aggregation of CPZ; (2) amphiphilic coassembly between anionic SC4AH and cationic CPZ. Both routes generate well-defined solid spherical assemblies with the desired CPZ loading efficiencies (61% and 46%).

Supra-amphiphile directed by SC4A-induced aggregation of CPZ

Recently, we proposed a novel strategy for the construction of supramolecular assemblies by means of CIA: complexation with *p*-sulfonatocalixarenes promotes the aggregation of aromatic or amphiphilic molecules by lowering the CAC, enhancing the aggregate stability, and regulating the degree of order in the aggregates.¹⁸

Before studying the aggregation of CPZ induced by complexation with calixarenes, it is necessary to know the aggregation behavior of free CPZ, which was examined by means of electrical conductivity measurements under the conditions used in this study (25 °C, aqueous solution at pH 7.0). The electrical conductivities of aqueous solutions of CPZ increased gradually as the concentration of CPZ was gradually increased from 10 to 270 μM, and an inflection point was obtained at the CPZ concentration of 140 μM, which implies typical amphiphilic aggregation. The CAC was estimated to be 140 μM (Fig. 1a). Dynamic light scattering (DLS) measurements for a 150 μM CPZ solution show no appreciable signal, indicating that CPZ does not tend to form large-sized aggregates at the CAC (Fig. 1b), but may form small micelles or oligomers.

When SC4A was added to the CPZ solution, the simple mixture of SC4A (50 μM) and CPZ (200 μM) in aqueous solution displayed the Tyndall effect, which prompted us to explore the higher-order hierarchy assembly based on the host-guest complexation of SC4A with CPZ. The CAC value of CPZ in the presence of 50 μM SC4A was measured by monitoring the dependence of the optical transmittance around 450 nm on the concentration of CPZ. In the presence of SC4A, the optical transmittance decreases gradually with increasing CPZ concentration as a result of amphiphilic assembly (Fig. 2a). The complexation-induced CAC value obtained was 125 μM

according to the plot of optical transmittance at 450 nm *versus* the CPZ concentration (Fig. 2b).

Determining the preferable mixing ratio between SC4A and CPZ is a prerequisite for fabricating a robust amphiphilic assembly. Fig. 3a shows the optical transmittance spectra of solutions with a fixed CPZ concentration of 150 μM and different SC4A concentrations. Interestingly, the transmittance undergoes a sharp decrease and then an inverse increase upon the gradual addition of SC4A. Plotting the transmittance at 450 nm *versus* the SC4A concentration (Fig. 3b), an inflection point was obtained at the SC4A concentration of 37.5 μM, corresponding to the SC4A/CPZ molar ratio of 0.25. It indicates that in the present SC4A-CPZ system, the best host-guest stoichiometry for amphiphilic aggregation is 1 : 4 SC4A to CPZ. In the left-hand portion of the inflection, SC4A and CPZ form a higher-order complex with a tendency to undergo amphiphilic aggregation, whereas in the right-hand portion of the inflection, excess SC4A leads to the formation of simple inclusion complexes accompanied by the disassembly of the amphiphilic aggregation. It is in good agreement with our previous results.^{17F-h,19a} Control experiments (Fig. 4) show that neither free SC4A nor CPZ lead to a decrease in transmittance. Additionally, replacing SC4A with its building subunit, 4-phenolsulfonic sodium, could not induce the formation of an assembly, which confirms the crucial role of the preorganized scaffold and cavity binding capability of SC4A in CIA. A clear Tyndall effect was detected in the SC4A-CPZ solution (Fig. 4), indicating the existence of an abundance of nanoparticles. However, no appreciable Tyndall effect was observed for either free SC4A, CPZ or 4-phenolsulfonic sodium-CPZ solution. These Tyndall results are in accordance with the above optical transmittance results, further validating that the formation of nanoscaled aggregates is undoubtedly directed by the host-guest complexation. Two driving factors are indispensable for CIA: (1) the host-guest inclusion interaction offered by the calixarene cavity and (2) the charge interactions between the upper-rim sulfonate groups of the host molecules and the charged groups of the guest molecules. On comparison with free CPZ, the aggregation behavior of the complexed CPZ underwent a pronounced change. This is because the intrinsic

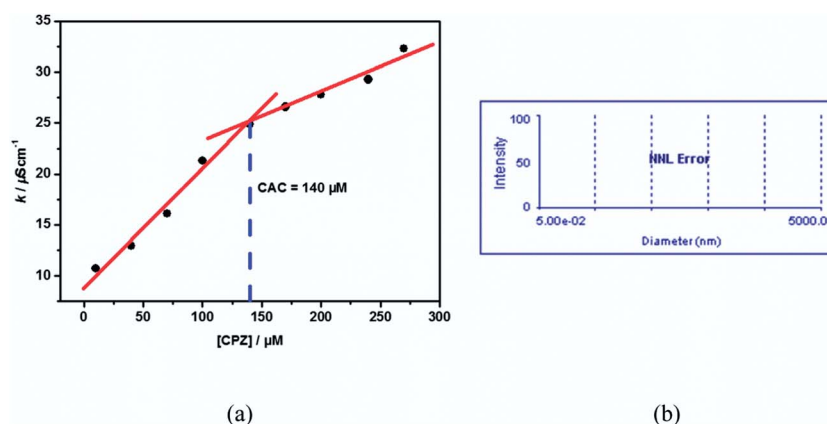


Fig. 1 (a) Dependence of electrical conductivity on the CPZ concentration in water (25 °C, pH 7.0). (b) DLS measurement of CPZ (150 μM).

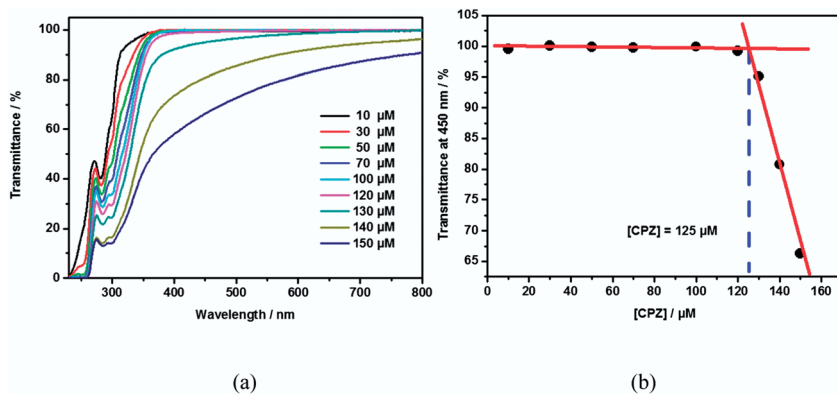


Fig. 2 (a) Optical transmittance of CPZ solutions at different concentrations in the presence of 50 μM SC4A and (b) the dependence of the optical transmittance at 450 nm on the CPZ concentration in the presence of 50 μM SC4A in water (25 $^{\circ}\text{C}$, pH 7.0).

electrostatic repulsion between the charged amino groups of the CPZ molecules was replaced by electrostatic attraction between the charged amino groups and the sulfonate groups of the SC4A molecules.

We postulate that the aggregation of CPZ induced by the complexation of SC4A occurred in two steps (Scheme 3). First, the host and guest molecules instantaneously formed a complex in which two CPZ molecules were captured by the cavities of two SC4A molecules, forming a 2 : 2 capsule-like complex driven by the host–guest interaction.²⁸ Subsequently, additional CPZ molecules were readily integrated into the 2 : 2 complexes, which resulted in the formation of compact aggregates. The resulting aggregates were simultaneously stabilized by several noncovalent interactions, including host–guest, charge, π -stacking, and hydrophobic interactions.

Furthermore, dynamic laser scattering (DLS) and transmission electron microscopy (TEM) were employed to identify the size and morphology of the self-assembled SC4A–CPZ complex. The concentrations of SC4A (37.5 μM) and CPZ (150 μM) were maintained in these experiments according to the aforementioned transmittance results. DLS results show that the SC4A–CPZ complex forms spectacular aggregates with a

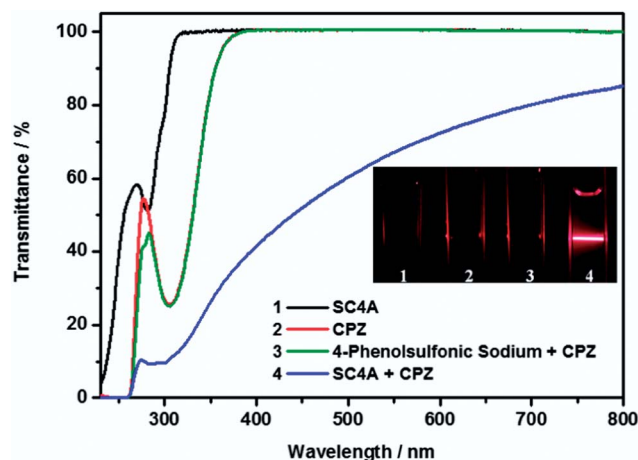


Fig. 4 Optical transmittance and Tyndall effect of free SC4A (1), free CPZ (2), CPZ–4-phenolsulfonic sodium (3), and SC4A–CPZ (4) in water (25 $^{\circ}\text{C}$, pH 7.0); [SC4A] = 37.5 μM , [CPZ] = 150 μM , [4-phenolsulfonic sodium] = 150 μM .

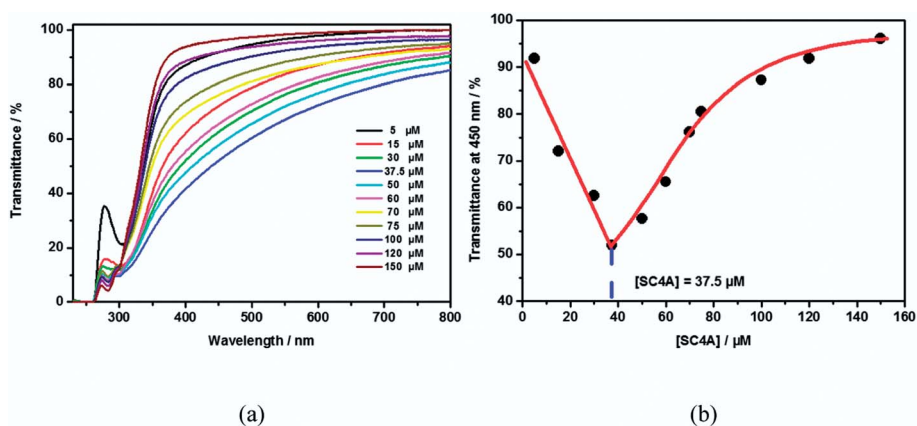
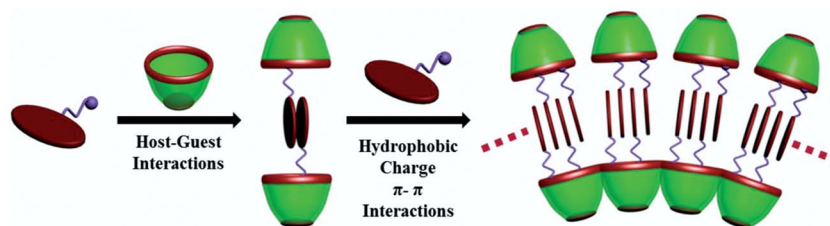


Fig. 3 (a) Optical transmittance of CPZ (150 μM) on increasing the SC4A concentration from 5 μM to 150 μM and (b) the dependence of the optical transmittance at 450 nm on the SC4A concentration with a fixed CPZ concentration of 150 μM in water (25 $^{\circ}\text{C}$, pH 7.0).



Scheme 3 Schematic illustration of CIA of CPZ.

narrow size distribution, giving an average diameter of 231 nm at a scattering angle of 90° (Fig. 5a). The formation of large-sized SC4A-CPZ aggregates was convincingly validated by TEM (Fig. 5b), which shows the spherical morphology. In order to determine the radial density distribution, the radius of gyration (R_g) and hydrodynamic radius (R_h) of the SC4A-CPZ complex were measured using light scattering studies. The ratio $\rho = R_g/R_h$ is a highly structure sensitive property, representing the radial density distribution of the particle.²⁹ Typical values of ρ are as follows: random coils $\rho = 1.5$ – 1.8 , solid spheres $\rho = 0.78$,²⁹ and hollow spheres with an infinitely thin shell $\rho = 1.0$.³⁰ The light scattering experiments at different scattering angles gave the radius of gyration ($R_g = 108$ nm) and hydrodynamic radius ($R_h = 141$ nm), respectively. The ratio $\rho = R_g/R_h = 0.77$ is characteristic of solid spheres. Combining all of the aforementioned results, we deduce that SC4A-CPZ nanoparticles exhibited typical amphiphilic characteristics and a bilayer structure that curved to generate multilamellar spheres. SC4A and CPZ are connected together by host-guest interactions. The phenothiazine rings in CPZ are π - π stacked together, and the intrinsic electrostatic repulsion between the charged amino groups of CPZ molecules was replaced by electrostatic attraction between the charged amino groups and the sulfonate groups of the SC4A molecules (Scheme 4).

To obtain the CPZ loading efficiency of the nanoparticles, the dispersion was ultracentrifuged, and the precipitates were analyzed by means of ^1H NMR (see the Experimental section). At a SC4A : CPZ mixing ratio of 1 : 4 ($[\text{SC4A}] = 37.5 \mu\text{M}$), the SC4A : CPZ molar ratio obtained in precipitates was 1 : 3.72, corresponding to a CPZ loading efficiency of 61%. The unchanged chemical composition of the nanoparticles could be attributed to the effective binary host-guest assembly.

The obtained supramolecular micelles have the capability of responding to the competitive binding of DBO with SC4A. Recently, we found that DBO is a favored guest molecule of SC4A with a strong binding affinity.²³ Here we have employed DBO as a competitive guest to replace CPZ in the cavities of SC4A, thereby leading to the disassembly of the micelle architecture. As shown in Fig. 6a, the transmittance of the SC4A-CPZ solution at 450 nm shows a pronounced increase upon the gradual addition of DBO. The Tyndall effect for the SC4A-CPZ solution (Fig. 6b, left) disappears after adding excess DBO (Fig. 6b, right).

Amphiphilic coassembly between anionic SC4AH and cationic CPZ

When compared with conventional amphiphiles, calixarene-based amphiphiles have lower CAC values and tend to present exchange rates several orders of magnitude slower, between monomers in bulk solution and in the aggregates.^{16a-c,e} Among calixarene-based amphiphiles described in the literature, *p*-sulfonatocalixarenes bearing alkyl groups at the lower rim were the first to be described and are probably the most studied.¹⁶

SC4AH, appended with the hydrophilic sulfonates at the upper rim of calix[4]arene and the hydrophobic *n*-heptyl chains at its lower rim, displays the desired amphiphilic nature. Since the intrinsic cone shape of calixarene is the prerequisite for high-curvature amphiphilic aggregation, SC4AH is expected to form a micellar assembly. We performed isothermal titration microcalorimetry (ITC) to investigate the aggregation of SC4AH (Fig. 7). The variation of ΔH_{obs} is plotted against the final concentration of SC4AH. The dilution curve is sigmoidal in shape, and can be subdivided into two concentration regions

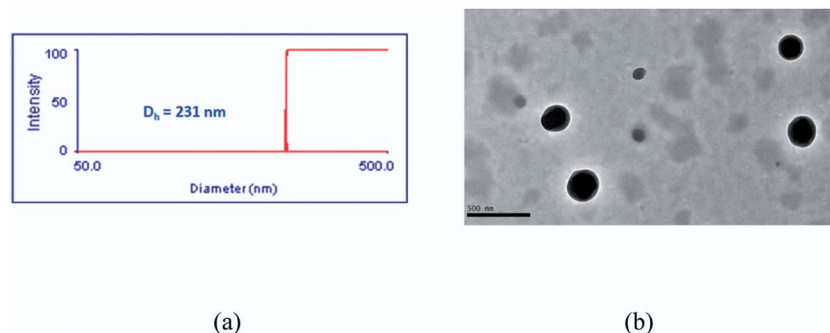
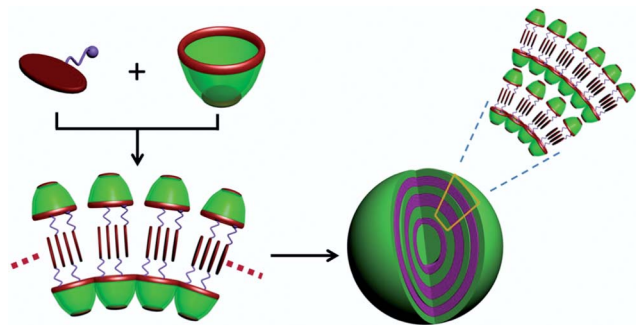


Fig. 5 (a) DLS data of the SC4A-CPZ assembly. (b) High-resolution TEM images of the SC4A-CPZ assembly (the scale bar is 500 nm).



Scheme 4 Models for the supra-amphiphile directed by SC4A-induced aggregation of CPZ.

separated by a transition region associated with micelle formation, corresponding to the CAC. When the concentration of SC4AH lies below the CAC, all added micelles are demicellized into monomers and the monomers are further diluted. When the concentration of SC4AH is above the CAC, only the micellar solution is diluted and the ΔH_{obs} drops toward zero. From such a titration curve, both the CAC value and the enthalpy change (ΔH_m) for micellization can be derived. As illustrated in Fig. 7, the fitted curve is differentiated with respect to the concentration of SC4AH and the position of the extremum is taken as the CAC ($210 \mu\text{M}$);³¹ the ΔH_m value ($-37.1 \text{ kJ mol}^{-1}$) is obtained from the titration curve by taking the enthalpy difference between the two linear segments of the enthalpy curve extrapolated to the CAC.³² The ΔH_m value is negative, which indicates that the micellization of SC4AH is exothermic. According to the previous results reported by Prof. García-Río,^{16f} three main factors are attributed to the micellization of SC4AH, which is similar to gemini amphiphiles: (1) the hydrophobic interactions, (2) van der Waals interactions, and (3) π - π interactions between the aromatic rings. The aggregation number of SC4AH at the CAC was calculated to be 13, corresponding to the small-sized aggregates which are not

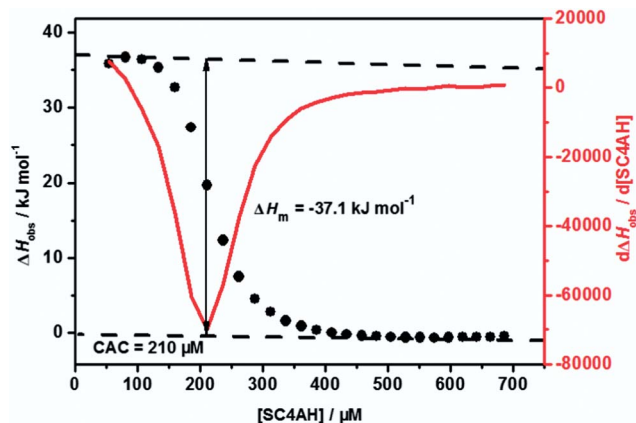


Fig. 7 Titration of 28 aliquots ($10 \mu\text{L}$) of $3.88 \times 10^3 \mu\text{M}$ solution of SC4AH into pure water at 298.15 K. Observed reaction enthalpy (ΔH_{obs}) versus the total SC4AH concentration in the reaction cell. The red line represents the first derivative of ΔH_{obs} against the concentration of SC4AH.

suitable for drug delivery due to their low drug loading efficiency. As proposed by Tanford,³³ two opposing forces are responsible for the formation of such amphiphilic assemblies. The hydrophobic effect drives the segregation of the alkyl chains in water, thus providing the impetus for self-organization. On the other hand, repulsive electrostatic forces between the polar headgroups prevent the formation of large three-dimensional assemblies. The coassembly of anionic and cationic amphiphiles (catanionic amphiphiles) is a fascinating system that offers an attractive approach to construct complex self-assembled nanostructures. The molecular self-assemblies of the catanionic amphiphiles are mainly attributed to the strong electrostatic attraction between the oppositely charged headgroups (ion-pair), which greatly promotes the dense packing of amphiphiles in the aggregate and results in a reduced headgroup area that causes spontaneous formation of stable and large assemblies.³⁴ Based on this strategy, we present

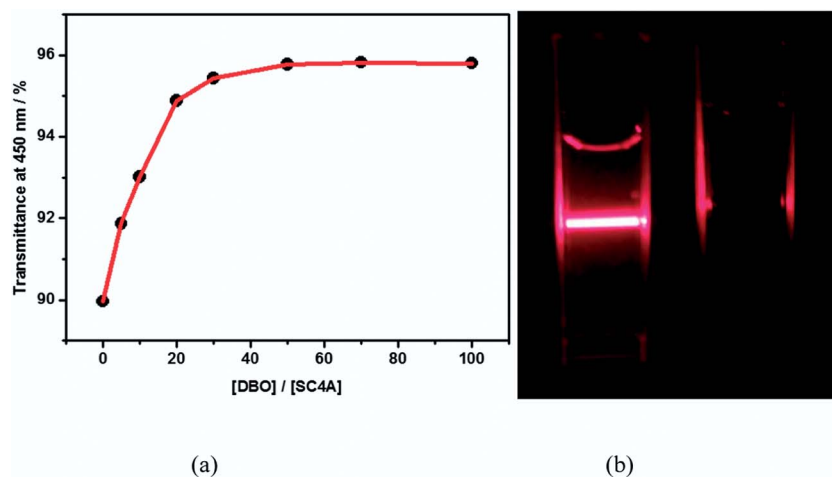


Fig. 6 (a) Dependence of the optical transmittance of the SC4A-CPZ solution at 450 nm on DBO concentration. (b) The Tyndall effect of the SC4A-CPZ solution in the absence (left) and in the presence (right) of excess DBO. [SC4A] = $20 \mu\text{M}$, [CPZ] = $80 \mu\text{M}$, [DBO] = $1000 \mu\text{M}$.

an amphiphilic coassembly between anionic SC4AH and cationic CPZ in this part.

The SC4AH : CPZ molar ratio was maintained at 1 : 3 in the following experiments because a precipitate was formed at the SC4AH : CPZ molar ratio of 1 : 4 (charge matching would generate unstable electroneutral micelles). Moreover, the 1 : 3 ratio leads to the formation of negatively charged micelles, which is favorable for the calixarene cavities at the outer-layer surface to capture positively charged functional ligands. As a result of amphiphilic aggregation, the optical transmittance decreased gradually with increasing concentration (Fig. 8a), and the CAC value of the SC4AH–CPZ complex was calculated to be 12 μM , which took the SC4AH concentration as standard according to the plot of optical transmittance at 450 nm (Fig. 8b). The concentrations of SC4AH (25 μM) and CPZ (75 μM) were maintained in the following experiments. A control experiment, replacing SC4AH with its building subunit 4-(heptyloxy)benzenesulfonate sodium, was performed (Fig. 9), and the optical transmittance exhibited no appreciable decrease. One possible reason is that the cyclic tetramer structure of SC4AH⁴⁻ could provide much stronger electrostatic attraction with CPZ than its building subunit. The SC4AH–CPZ solution exhibited a clear Tyndall effect (Fig. 9), indicating the existence of an abundance of nanoparticles. However, neither free SC4AH solution, CPZ solution nor 4-(heptyloxy)benzenesulfonate–CPZ sodium solution exhibited a similar Tyndall effect, revealing not only that neither free SC4AH nor CPZ can form nanoscale aggregates under the same conditions, but also that replacing SC4AH with its building subunit 4-(heptyloxy)benzenesulfonate sodium cannot induce the formation of nanoscale aggregates, which is in accordance with the above optical transmittance results.

DLS and TEM were employed to identify the assembly size and morphology of the SC4AH–CPZ complex. In DLS measurements, particles formed by the complex exhibit an average diameter of 192 nm at a scattering angle of 90° (Fig. 10a). The TEM image shows the spherical particles (Fig. 10b). The light scattering studies at different scattering angles also revealed the radius of gyration ($R_g = 81$ nm) and hydrodynamic radius ($R_h = 101$ nm). The ratio $\rho = R_g/R_h = 0.80$ is characteristic for solid spheres. Furthermore, the nanoparticles were found to possess a zeta potential of -16.18 mV. The negative value is reasonably acceptable according to the mixing ratio of 1 : 3 (SC4AH⁴⁻ : CPZ⁺)

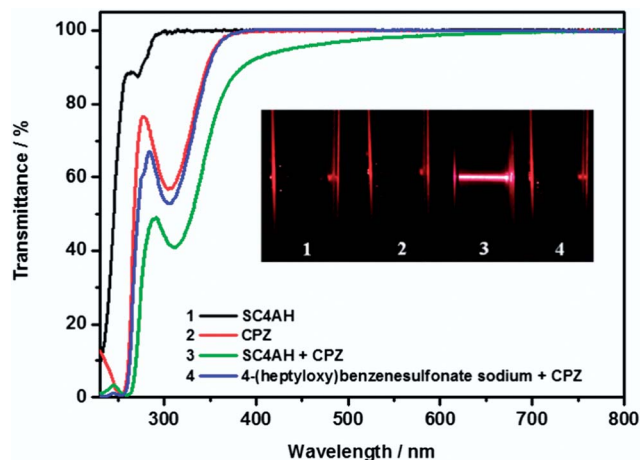


Fig. 9 Optical transmittance and Tyndall effect of free SC4AH (1), free CPZ (2), SC4AH–CPZ (3), and 4-(heptyloxy)benzenesulfonate sodium–CPZ (4) in water (25 °C, pH 7.0); [SC4AH] = 25 μM , [CPZ] = 75 μM , [4-(heptyloxy)benzenesulfonate sodium] = 100 μM .

and further indicates that the sulfonate groups of SC4AH were on the surfaces of the nanoparticles. Combining all of the aforementioned results, we deduce that SC4AH–CPZ forms multilamellar spherical micelles (Scheme 5). The strong electrostatic attraction between the oppositely charged headgroups (ion-pair) of SC4AH and CPZ greatly promotes their dense packing in the aggregates and results in a reduced headgroup area, which causes the spontaneous formation of stable and large assemblies. CPZ plays an important role in the construction of micelles as a pharmaceutical subunit.

We used the same method mentioned above to obtain the CPZ loading efficiency in the SC4AH–CPZ nanoparticles. At a SC4AH : CPZ mixing ratio of 1 : 3 ([SC4AH] = 25 μM), the SC4AH : CPZ molar ratio in precipitates was 1 : 2.96, corresponding to a CPZ loading of 46%. The unchanged chemical composition of the nanoparticles could be attributed to the electrostatic attraction between the oppositely charged headgroups of SC4AH and CPZ, which promoted their dense packing in the nanoparticles.

Owing to the host–guest recognition site of SC4AH on the outer surface of the SC4AH–CPZ particles, a variety of targeting ligands, diagnostic probes and therapeutic cargos could be

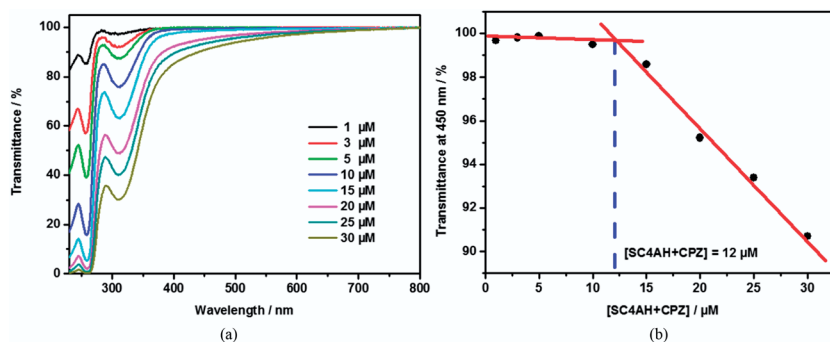
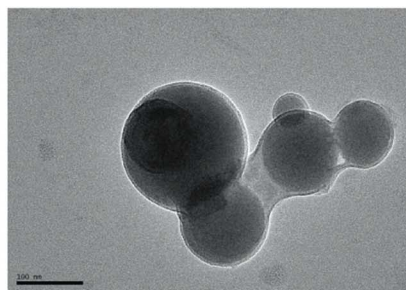
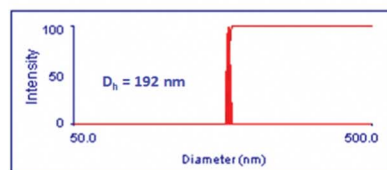


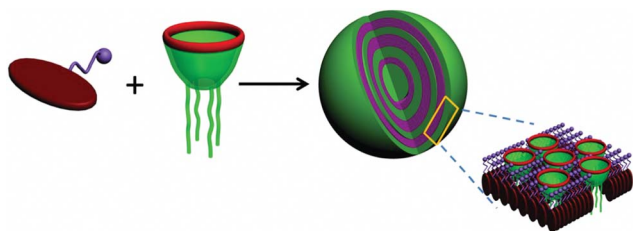
Fig. 8 (a) Optical transmittance of the SC4AH–CPZ complex by increasing the concentration from 1 μM to 30 μM and (b) dependence of the optical transmittance at 450 nm on the complex concentration in water (25 °C, pH 7.0).



(a)

(b)

Fig. 10 (a) DLS data of the SC4AH-CPZ assembly. (b) High-resolution TEM images of the SC4AH-CPZ assembly (the scale bar is 100 nm).



Scheme 5 Models for amphiphilic coassembly between anionic SC4AH and cationic CPZ.

further non-covalently anchored on them. Trimethylated chitosan (TMC) is a permanently quaternized chitosan derivative which is positively charged under physiological conditions.³⁵ It is a water soluble, non-toxic material which has great advantages as a targeting agent. As a cationic ligand, TMC can facilitate the active transport of nanoparticles *via* absorptive-mediated transcytosis. Therefore, TMC-modified nanoparticles could be used as a drug carrier for delivery to the brain.^{36,37} The zeta potential of the SC4AH-CPZ particles changed from -16.18 mV to -7.28 mV upon the addition of TMC, indicating that TMC was captured on the surface of the SC4AH-CPZ particles *via* host-guest interactions between the calixarene cavities and quaternary ammonium ions. As a result, these TMC coated SC4AH-CPZ particles may lead to potential applications in targeted drug delivery.

Conclusion

In summary, we constructed two amphiphilic assemblies based on the non-covalent interaction between anionic *p*-sulfonato-calixarenes and cationic CPZ *via* two different assembling models: (1) supra-amphiphile directed by SC4A-induced aggregation of CPZ; (2) amphiphilic coassembly between anionic SC4AH and cationic CPZ. Both routes generate large-sized multilamellar spherical micelles which cannot be achieved by using any component alone. CPZ itself acts as an essential building subunit that leads to the desired high loading efficiencies (61% and 46%). Furthermore, due to the host-guest recognition site of SC4AH on the outer-layer surface, a targeting

agent, TMC, could be further non-covalently anchored on the SC4AH-CPZ nanoparticles for targeted delivery. Our strategy of calixarene-drug coassembly thus provides a new direction for the development of carriers with high drug loading and easy processability. The versatility of the envisaged nanoconstructs, simply by changing the drug molecule and the exposed ligand, may be a highly desirable advantage for engineering a universal nanocarrier.

Notes

The authors declare no competing financial interest.

Acknowledgements

We thank the 973 Program (2011CB932502), and the NNSFC (no. 91227107, 21172119 and 21322207) for the financial support.

References

- 1 V. P. Torchilin, *Nat. Rev. Drug Discovery*, 2005, **4**, 145–160.
- 2 V. V. Ranade, *J. Clin. Pharmacol.*, 1990, **30**, 10–23.
- 3 A. Samad, M. I. Alam and K. Saxena, *Curr. Pharm. Des.*, 2009, **15**, 2958–2969.
- 4 M. Liang, J. Lu, M. Kovoichich, T. Xia, S. G. Ruehm, A. E. Nel, F. Tamanoi and J. I. Zink, *ACS Nano*, 2008, **2**, 889–896.
- 5 E. C. Mary, B. L. William and A. P. Nicholas, *Acc. Chem. Res.*, 2011, **44**, 1061–1070.
- 6 R. Duncan, *Nat. Rev. Cancer*, 2006, **6**, 688–701.
- 7 J. P. K. Tan, S. H. Kim, F. Nederberg, E. A. Appel, R. M. Waymouth, Y. Zhang, J. L. Hedrick and Y. Y. Yang, *Small*, 2009, **5**, 1504–1507.
- 8 (a) C. Párkányi, C. Boniface, J. J. Aaron and M. Maafi, *Spectrochim. Acta*, 1993, **12**, 1715–1720; (b) J. M. Ford and W. N. Hait, *Pharmacol. Rev.*, 1990, **42**, 155–199; (c) G. J. S. Fowler, R. C. Rees and R. Devonshire, *Photochem. Photobiol.*, 1990, **52**, 489–494; (d) A. Ramu and N. Ramu, *Cancer Chemother. Pharmacol.*, 1992, **30**, 165–173.
- 9 D. Attwood, *Adv. Colloid Interface Sci.*, 1995, **55**, 271–303.

- 10 M.-Z. Asfari, V. Böhmer, J. Harrowfield and J. Vicens, *Calixarenes*, Kluwer Academic Publishers, Dordrecht, 2001.
- 11 A. Mulder, T. Auletta, A. Sartori, S. D. Ciotto, A. Casnati, R. Ungaro, J. Huskens and D. N. Reinhoudt, *J. Am. Chem. Soc.*, 2004, **126**, 6627–6636.
- 12 A. Arduini, D. Demuru, A. Pochini and A. Secchi, *Chem. Commun.*, 2005, 645–647.
- 13 A. Arduini, F. Ciesa, M. Fragassi, A. Pochini and A. Secchi, *Angew. Chem., Int. Ed.*, 2005, **44**, 278–281.
- 14 D. M. Rudkevich, *Bull. Chem. Soc. Jpn.*, 2002, **75**, 393–413.
- 15 K. Helttunen and P. Shahgaldian, *New J. Chem.*, 2010, **34**, 2704–2714.
- 16 (a) S. Shinkai, S. Mori, H. Koreishi, T. Tsubake and O. Manabe, *J. Am. Chem. Soc.*, 1986, **108**, 2409–2416; (b) S. Shinkai, H. Kawabata, T. Arimura, T. Matsuda, H. Satoh and O. Manabe, *J. Chem. Soc., Perkin Trans. 1*, 1989, 1073–1074; (c) S. Shinkai, T. Arimura, K. Araki, H. Kawabata, H. Satoh, T. Tsubaki, O. Manabe and J. Sunamoto, *J. Chem. Soc., Perkin Trans. 1*, 1989, 2039–2045; (d) S. Arimori, T. Nagasaki and S. Shinkai, *J. Chem. Soc., Perkin Trans. 2*, 1995, 679–683; (e) N. Basílio, L. García-Río and M. Martín-Pastor, *J. Phys. Chem. B*, 2010, **114**, 4816–4820; (f) N. Basílio and L. García-Río, *ChemPhysChem*, 2012, **13**, 2368–2376; (g) N. Basílio, L. García-Río and M. Martín-Pastor, *Langmuir*, 2012, **28**, 2404–2414; (h) F. Sansone, M. Dudic, G. Donofrio, C. Rivelli, L. Baldini, A. Casnati, S. Cellai and R. Ungaro, *J. Am. Chem. Soc.*, 2006, **128**, 14528–14536; (i) G. M. L. Consoli, G. Granata, R. L. Nigro, G. Malandrino and C. Geraci, *Langmuir*, 2008, **24**, 6194–6200.
- 17 The definition of supra-amphiphiles is proposed by X. Zhang, see: (a) X. Zhang and C. Wang, *Chem. Soc. Rev.*, 2011, **40**, 94–101; (b) C. Wang, Z. Q. Wang and X. Zhang, *Acc. Chem. Res.*, 2012, **45**, 608–618; (c) K. Liu, Y. X. Yao, C. Wang, Y. Liu, Z. B. Li and X. Zhang, *Chem.–Eur. J.*, 2012, **18**, 8622–8628; (d) Y. B. Xing, C. Wang, P. Han, Z. Q. Wang and X. Zhang, *Langmuir*, 2012, **28**, 6032–6036; (e) K. Liu, Y. X. Yao, Y. Liu, C. Wang, Z. B. Li and X. Zhang, *Langmuir*, 2012, **28**, 10697–10702. Recent researches on the calixarene-based supra-amphiphiles: (f) K. Wang, D.-S. Guo and Y. Liu, *Chem.–Eur. J.*, 2010, **16**, 8006–8011; (g) K. Wang, D.-S. Guo and Y. Liu, *Chem.–Eur. J.*, 2012, **18**, 8758–8764; (h) D.-S. Guo, K. Wang, Y.-X. Wang and Y. Liu, *J. Am. Chem. Soc.*, 2012, **134**, 10244–10250; (i) V. Francisco, N. Basílio, L. García-Río, J. R. Leis, E. F. Maques and C. Vázquez-Vázquez, *Chem. Commun.*, 2010, **46**, 6551–6553; (j) N. Basílio, M. Martín-Pastor and L. García-Río, *Langmuir*, 2012, **28**, 6561–6568; (k) N. Basílio, B. Gómez, L. García-Río and V. Francisco, *Chem.–Eur. J.*, 2013, **19**, 4570–4576; (l) N. Basílio, V. Francisco and L. García-Río, *Int. J. Mol. Sci.*, 2013, **14**, 3140–3157; (m) C. Bize, J.-C. Garrigues, M. Blanzat, I. Rico-Lattes, O. Bistri, B. Colasson and O. Reinaud, *Chem. Commun.*, 2010, **46**, 586–588; (n) S. Houmadi, D. Coquière, L. Legrand, M. C. Fauré, M. Goldmann, O. Reinaud and S. Rémita, *Langmuir*, 2007, **23**, 4849–4855; (o) C. L. Tu, L. J. Zhu, P. P. Li, Y. Chen, Y. Su, D. Y. Yan, X. Y. Zhu and G. Y. Zhou, *Chem. Commun.*, 2011, **47**, 6063–6065.
- 18 (a) D.-S. Guo, B.-P. Jiang, X. Wang and Y. Liu, *Org. Biomol. Chem.*, 2012, **10**, 720–723; (b) Z. Q. Li, C. X. Hu, Y. Q. Cheng, H. Xu, X. L. Cao, X. W. Song, H. Y. Zhang and Y. Liu, *Sci. China: Chem.*, 2012, **55**, 2063–2068; (c) F. G. Gulino, R. Lauceri, L. Frish, T. Evan-Salem, Y. Cohen, R. D. Zorzi, S. Geremia, L. D. Costanzo, L. Randaccio, D. Sciotto and R. Purrello, *Chem.–Eur. J.*, 2006, **12**, 2722–2729; (d) V. Lau and B. Heyne, *Chem. Commun.*, 2010, **46**, 3595–3597.
- 19 (a) K. Wang, D.-S. Guo, X. Wang and Y. Liu, *ACS Nano*, 2011, **5**, 2880–2894; (b) Y.-X. Wang, D.-S. Guo, Y. Cao and Y. Liu, *RSC Adv.*, 2013, **3**, 8058–8063; (c) M. Lee, S.-J. Lee and L.-H. Jiang, *J. Am. Chem. Soc.*, 2004, **126**, 12724–12725; (d) E.-H. Ryu and Y. Zhao, *Org. Lett.*, 2004, **6**, 3187–3189; (e) Y. Tauran, A. Brioude, P. Shahgaldian, A. Cumbo, B. Kim, F. Perret, A. W. Coleman and I. Montasser, *Chem. Commun.*, 2012, **48**, 9483–9485; (f) V. Wintgens, C. L. Coeur, C. Amiel, J.-M. Guigner, J. G. Harangozó, Z. Miskolczy and L. Biczók, *Langmuir*, 2013, **29**, 7682–7688; (g) S. Fujii, Y. Sanadsa, T. Nishimura, I. Akiba and K. Sakurai, *Langmuir*, 2012, **28**, 3092–3101; (h) P. K. Eggers, T. Becker, M. K. Melvin, R. A. Boulos, E. James, N. Morellini, A. R. Harvey, S. A. Dunlop, M. Fitzgerald, K. A. Stubbs and C. L. Raston, *RSC Adv.*, 2012, **2**, 6250–6257.
- 20 I. Hyejae, K. Hyunjun and P. Kyungsoo, *J. Chem. Soc., Perkin Trans. 1*, 1997, 1997–2004.
- 21 G. Arena, A. Contino, G. G. Lombardo and D. Sciotto, *Thermochim. Acta*, 1995, **264**, 1–11.
- 22 E. Mary, Z. Barbara, R. Michael, J. Stanley, L. Darrin and B. Ram, *Mol. Cryst. Liq. Cryst.*, 1988, **154**, 209–240.
- 23 H.-X. Zhao, D.-S. Guo and Y. Liu, *J. Phys. Chem. B*, 2013, **117**, 1978–1987.
- 24 (a) J. H. Park, S. Lee, J.-H. Kim, K. Park, K. Kim and I. C. Kwon, *Prog. Polym. Sci.*, 2008, **33**, 113–137; (b) S. Cavalli, F. Albericio and A. Kros, *Chem. Soc. Rev.*, 2010, **39**, 241–263; (c) F. Sallas and R. Darcy, *Eur. J. Org. Chem.*, 2008, 957–969; (d) G. W. Gokel, W. M. Leevy and M. E. Weber, *Chem. Rev.*, 2004, **104**, 2723–2750.
- 25 (a) J. N. Israelachvili, *Intermolecular and Surface Forces*, Academic Press, New York, 1985; (b) M. Kellermann, W. Bauer, A. Hirsch, B. Schade, K. Ludwig and C. Böttcher, *Angew. Chem., Int. Ed.*, 2004, **43**, 2959–2962.
- 26 (a) D.-S. Guo, K. Wang and Y. Liu, *J. Inclusion Phenom. Macroyclic Chem.*, 2008, **62**, 1–21; (b) F. Perret and A. W. Coleman, *Chem. Commun.*, 2011, **47**, 7303–7319; (c) F. Perret, A. N. Lazar and A. W. Coleman, *Chem. Commun.*, 2006, 2425–2438.
- 27 O. Danylyuk and K. Suwinska, *Chem. Commun.*, 2009, 5799–5813.
- 28 Aggregation of CPZ at concentrations below its CAC is well described and the structure of a dimer has been presented. (a) D. Attwood, E. Boitard, J. P. Dubes and H. Tachoire, *J. Phys. Chem.*, 1992, **96**, 11018–11021; (b) D. Attwood, R. Waigh, R. Blundell, D. Bloor, A. Thevand, E. Boitard, J. P. Dubes and H. Tachoire, *Magn. Reson. Chem.*, 1994, **32**, 468–472.
- 29 W. Burchard, *Adv. Polym. Sci.*, 1983, **48**, 1–124.

- 30 W. Egelhaaf, *Physical Techniques for the Study of Food Biopolymers*, Blackie Academics & Professional, Glasgow, 1994.
- 31 Z. Király and I. Dekány, *J. Colloid Interface Sci.*, 2001, **242**, 214–219.
- 32 I. Johnson, G. Olofsson and B. Jönsson, *J. Chem. Soc., Faraday Trans. 1*, 1987, **83**, 3331–3344.
- 33 C. Tanford, *The Hydrophobic Effect: Formation of Micelles and Biological Membranes*, John Wiley & Sons Inc., New York, 1973.
- 34 (a) Y. Lin, X. Han, X. Cheng, J. Huang, D. Liang and C. Yu, *Langmuir*, 2008, **24**, 13918–13924; (b) J. Park, L. H. Rader, G. B. Thomas, E. J. Danoff, D. S. English and P. DeShong, *Soft Matter*, 2008, **4**, 1916–1921; (c) H. Li, J. Hao and Z. Wu, *J. Phys. Chem. B*, 2008, **112**, 3705–3710; (d) F. M. Menger and L. Shi, *J. Am. Chem. Soc.*, 2009, **131**, 6672–6673.
- 35 M. Amidi, S. G. Romeijn, G. Borchard, H. E. Junginger, W. E. Hennink and W. Jiskoot, *J. Controlled Release*, 2006, **111**, 107–116.
- 36 U. Bickel, T. Yoshikawa and W. M. Pardridge, *Adv. Drug Delivery Rev.*, 2001, **46**, 247–279.
- 37 W. Lu, Y. Zhang, Y. Z. Tan, K. L. Hu, X. G. Jiang and S. K. Fu, *J. Controlled Release*, 2005, **107**, 428–448.